

Original Article

Short-term Calorie Restriction and 17α -Estradiol Administration Elicit Divergent Effects on Proteostatic Processes and Protein Content in Metabolically Active Tissues

Benjamin F. Miller, PhD,¹ Gavin A. Pharaoh, BS,^{1,2} Karyn L. Hamilton, PhD,³ Fredrick F. Peelor III, BS,¹ James L. Kirkland, MD, PhD,⁴ Willard M. Freeman, PhD,^{2,5,6} Shivani N. Mann, BS,^{5,7} Michael Kinter, PhD,¹ John C. Price, PhD,⁸ and Michael B. Stout, PhD^{5,7,*}

¹Aging and Metabolism Research Program, Oklahoma Medical Research Foundation. ²Department of Physiology, University of Oklahoma Health Sciences Center. ³Health and Exercise Science Department, Colorado State University, Fort Collins. ⁴Robert and Arlene Kogod Center on Aging, Mayo Clinic, Rochester, Minnesota. ⁵Reynolds Oklahoma Center on Aging, University of Oklahoma Health Sciences Center. ⁶Oklahoma City Veterans Affairs Medical Center. ⁷Department of Nutritional Sciences, University of Oklahoma Health Sciences Center. ⁸Department of Chemistry and Biochemistry, Brigham Young University, Provo, Utah.

*Address correspondence to: Michael B. Stout, Department of Nutritional Sciences, University of Oklahoma Health Sciences Center, 1200 N Stonewall Ave, Suite 3057, Oklahoma City, OK 73117. E-mail: michael-stout@ouhsc.edu

Decision Editor: Rozalyn Anderson, PhD

Received: January 7, 2019; Editorial Decision Date: April 29, 2019

Abstract

17α -Estradiol (17α -E2) is a “non-feminizing” estrogen that extends life span in male, but not female, mice. We recently reported that 17α -E2 had robust beneficial effects on metabolic and inflammatory parameters in aged male mice. However, it remains unclear if 17α -E2 also delays other “hallmarks” of aging, particularly maintaining proteostasis. Here, we used isotope labeling methods in older mice to examine proteostatic mechanisms. We compared weight-matched mild calorie restricted (CR) and 17α -E2 treated male mice with the hypothesis that 17α -E2 would increase protein synthesis for somatic maintenance. 17α -E2 had no effect on protein synthesis or DNA synthesis in multiple tissues, including white adipose tissue. Conversely, mild short-term CR decreased DNA synthesis and increased the protein to DNA synthesis ratio in multiple tissues. Examination of individual protein synthesis and content did not differentiate treatments, although it provided insight into the regulation of protein content between tissues. Contrary to our hypothesis, we did not see the predicted differences in protein to DNA synthesis following 17α -E2 treatment. However, mild short-term CR elicited differences consistent with both lifelong CR and other treatments that curtail aging processes. These data indicated that despite similar maintenance of body mass, 17α -E2 and CR treatments elicit distinctly different proteostatic outcomes.

Keywords: Protein synthesis, Proteomics, Deuterium oxide, Mouse, Metabolism

The aging process and onset of age-related diseases can be delayed by dietary interventions that modulate metabolic signaling pathways, such as caloric restriction (CR) (1). In addition to dietary interventions, several orally consumed compounds, such as those tested by the National Institute on Aging Interventions Testing Program, have also shown promise as interventional strategies to curtail disease and/or extend longevity (2). One of the more recently

studied compounds to demonstrate benefits on health parameters and longevity is 17α -estradiol (17α -E2). 17α -E2 is a naturally occurring enantiomer of 17β -estradiol that has long been considered “non-feminizing” due to its weak affinity for classical estrogen receptors (3,4). The National Institute on Aging Interventions Testing Program has reported that 17α -E2 extends life span in male, but not female, mice at two different doses (4.8 and 14.4 ppm) (5,6).

The higher dose, which was started at 10 months of age, increased median life span by 19% in male mice (6). In alignment with these findings, we recently reported that 17 α -E2 had robust beneficial effects on metabolic and inflammatory parameters in aged male mice as evidenced by decreased adiposity, improved insulin sensitivity, and reduced pro-inflammatory cytokines and chemokines in white adipose tissue (WAT) and the circulation (7). These observations were also associated with changes in WAT AMPK α and mTORC1 signaling, which are consistent with beneficial metabolic outcomes with advancing age (8,9). Interestingly, we have also reported that 17 α -E2 has profound effects on adiposity in middle-aged obese male mice (10), suggesting that 17 α -E2 may have direct actions in WAT.

Garratt and colleagues (11) have also assessed several metabolic-related variables in mice receiving 17 α -E2. The authors did not assess changes in body mass or adiposity in this study but did report enhanced glucose tolerance, insulin sensitivity, and mTORC2 signaling in male mice receiving 17 α -E2, all of which are markers of improved metabolic homeostasis (12). In a subsequent report, Garratt and colleagues also provided evidence that 17 α -E2 likely modifies hepatic amino acid metabolism in male mice (13), which further implicates metabolic regulation in 17 α -E2-mediated effects. Collectively, all of the aforementioned studies suggest that the mechanisms responsible for improvements in health span and longevity by 17 α -E2 are closely aligned with alterations of metabolic homeostasis. However, it remains unclear if 17 α -E2 also delays other “hallmarks” of aging, particularly maintaining proteostasis given its apparent regulation of the mTOR protein complexes (7,11).

Proteostasis is a central player in aging biology in that it contributes to somatic maintenance (14). Protein turnover is one of the primary mechanisms for maintaining proteostasis (15) and could be a key strategy for preserving proteome fidelity and slowing the aging process (16). We have focused on the trade-off between growth (marked by cellular proliferation) and somatic maintenance (17,18) in accelerated or slowed aging conditions (14). To do so, we measure protein and DNA synthesis to account for protein synthesis being directed toward proliferation and growth, versus protein synthesis to maintain existing cellular structures. When cells proliferate, DNA replicates and protein mass doubles so that new cells have the full complement of both nuclear material and proteins (19). Thus, cellular proliferation increases the rates of both protein and DNA synthesis. In contrast, cell remodeling only requires a change in protein turnover without a change in DNA synthesis. Protein synthesis for growth is thought to exacerbate aging processes, whereas protein synthesis for somatic maintenance is thought to slow aging processes (14,17,18). Our studies assessing both protein and DNA synthesis consistently demonstrate greater activation of proteostatic mechanisms in long-lived models. Specifically, mice undergoing lifelong CR, the Snell Dwarf, rapamycin-treated, crowded litter, and Nrf2 activator-treated mice display greater protein to DNA synthesis rates than that of controls (18,20–22). These findings reflect an energetic trade-off in these models, in which greater proteostatic regulation is maintained for the purpose of somatic maintenance at the cost of cellular proliferation and growth (17). Despite the abundance of data demonstrating that 17 α -E2 improves a variety of metabolic variables (7,10,11), it remains unclear if this treatment modality may also be affecting cellular proliferation and proteostasis when administered late in life. Similarly, we do not know if short-term, mild CR has similar protein turnover responses as those observed with lifelong 40% CR.

The purpose of the current analyses was to compare and contrast proteostatic mechanisms in peripheral tissues from weight-matched

old male mice undergoing 17 α -E2 or short-term mild CR. We chose to analyze peripheral metabolically active tissues because previous studies indicate significant effects of CR and 17 α -E2 in these organs. We hypothesized that CR and 17 α -E2 would modulate proteostatic processes in a similar fashion. Herein, we report the first simultaneous assessment of protein and DNA synthesis rates in WAT, which is known to serve an important role in modulating systemic metabolic homeostasis and aging processes (23,24). In addition, we performed targeted quantitative and kinetic proteomic assessments of key enzymes involved in metabolic processes in several tissues to determine how turnover may be affected by late-life CR or 17 α -E2. Contrary to our hypothesis, 17 α -E2 treated mice displayed no changes in protein to DNA synthesis rates in any tissue, whereas late-life CR did modify this ratio in a manner similar to a life-long intervention (18). Furthermore, tissue-specific differences in the regulation of individual protein synthetic rates were observed following CR. These findings indicate that proteostatic mechanisms are differentially modulated by some, but not all, life span-extending interventions.

Methods

Animals

All animal procedures were reviewed and approved by the institutional animal care and use committees. All mice (male C57BL/6) were obtained from the National Institute on Aging and were individually housed at 24 \pm 0.5°C on a 12:12-hour light–dark cycle. Unless otherwise noted, mice had ad libitum access to food and water throughout the experiment. Twenty-month-old mice (7–10 per group) were randomized by body mass, body composition, fasting glucose, and Hemoglobin A1c (HbA1c) to control (CON), 17 α -E2, or CR treatment groups, as reported previously (7). Body mass and food intake were measured daily, whereas body composition was measured weekly throughout the 5-week intervention by quantitative magnetic resonance using an EchoMRI-100H analyzer (data previously reported in ref. (7)). Daily food allotment for the CR treatment group was calculated based on body mass changes in the 17 α -E2 treatment group from the previous day. LabDiet 58YP (66.4% CHO, 20.5% PRO, 13.1% FAT) was used as the CON and CR diet and was supplemented with 17 α -E2 (14.4 ppm; Steraloids, Newport, RI) for the treatment diet (TestDiet; Richmond, IN). This design allowed for weight-matching between the 17 α -E2 and CR treatment groups and averaged approximately 18% restriction compared with controls over the course of the study. The CR mice received half of their daily food allotment at 0600 hour and the remainder at 1800 hour.

The use of $^2\text{H}_2\text{O}$ (D_2O) allows simultaneous assessment of multiple synthetic processes. Here, we assessed the synthesis of mitochondrial (mito), cytosolic (cyto), and mixed (mixed) proteins and DNA in WAT, liver, and cardiac tissues according to procedures described previously, which were modified for WAT analysis (see later). Two weeks before killing the mice received an intraperitoneal injection of 99% enriched D_2O calculated to enrich the body water pool (assumed 60% of body weight) to 5%. Animals were then allowed to drink ad libitum water enriched to 8% for the next 2 weeks (20,21,25–27). At the conclusion of the study, mice were anesthetized with isoflurane and euthanized by cervical dislocation before dissection. Blood was collected into ethylenediaminetetraacetic acid-lined tubes by cardiac puncture and plasma was collected and frozen. Tissues were excised, weighed, flash-frozen, and stored at -80°C . For isotope studies, inguinal WAT was used as a representative subcutaneous depot, whereas the subscapular WAT was used

as a representative subcutaneous depot for quantitative proteomics. The quadriceps muscle was used as the skeletal muscle sample.

Isotopic Labeling Study Design and Analysis

For protein isolation, tissues were fractionated according to our previously published procedures (20,21,25–27). Heart and liver were homogenized 1:10 in isolation buffer (100 mM KCl, 40 mM Tris–HCl, 10 mM Tris Base, 5 mM MgCl₂, 1 mM ethylenediaminetetraacetic acid, 1 mM ATP, pH = 7.5) with phosphatase and protease inhibitors (HALT, Thermo Scientific, Rockford, IL) using a bead homogenizer (Next Advance Inc., Averill Park, NY). WATs were homogenized 1:5 in isolation buffer using a handheld homogenizer (Fisher Scientific, Hampton, NH). The supernatant from homogenized WATs was spun and transferred 3× in an effort to eliminate the vast majority of lipid from these samples. After homogenization, subcellular fractions were isolated via differential centrifugation as described previously (20,21,25–27). Once protein pellets were isolated and purified, 250 µL 1 M NaOH was added and pellets were incubated for 15 minutes at 50°C with slowly mixing. For DNA analysis, DNA was extracted from approximately 20 mg of tissue or bone marrow suspension (QIAamp DNA Mini Kit Qiagen, Valencia, CA). Protein was hydrolyzed by incubation for 24 hours at 120°C in 6 N HCl. The pentafluorobenzyl-*N,N*-di(pentafluorobenzyl) derivative of alanine was analyzed on an Agilent 7890A GC coupled to an Agilent 5975C MS as described previously (20,21,25–27).

To determine body water enrichment, 125 µL plasma was placed into the inner well of o-ring screw cap and inverted on heating block overnight to collect distilled water at the top. Two microliter 10 M NaOH and 20 µL acetone were added to all distilled samples and to 20 µL 0%–20% D₂O standards and then capped immediately. Samples were vortexed at low speed and left at room temperature overnight. Extraction was performed by the addition of 200 µL hexane. The organic layer was transferred through anhydrous Na₂SO₄ into GC vials and analyzed via EI mode.

Determination of ²H incorporation into purine deoxyribose (dR) of DNA was performed as described previously (20,21,25). Briefly, DNA isolated from heart, liver, bone marrow, and WATs were hydrolyzed overnight at 37°C with nuclease S1 and potato acid phosphatase. Hydrolysates were reacted with pentafluorobenzyl hydroxylamine and acetic acid and then acetylated with acetic anhydride and 1-methylimidazole. Dichloromethane extracts were dried, resuspended in ethyl acetate, and analyzed by GC/MS as described previously (20,21,25).

The newly synthesized fraction (fraction new) of proteins and DNA were calculated from the product enrichment divided by the true precursor enrichment using plasma analyzed for D₂O enrichment and adjusted according to mass isotopomer distribution analysis, or bone marrow as a fully turned over DNA pool (28,29). The fraction new was divided by time and expressed as fractional synthesis rates (%/day). The ratio of protein synthesis to DNA synthesis (protein/DNA) was calculated as an indicator of proteostatic mechanisms (17,18,20).

Targeted Quantitative Proteomics and Kinetic Proteomics: Targeted Quantitative Proteomics and Kinetic Proteomics

Quantitative proteomics was performed using high-resolution accurate mass measurements on a ThermoScientific Q-Exactive Plus targeting selected and validated peptides from each protein measured. In brief, 20 µg of total tissue homogenates were run 1.5 cm into

a 12.5% sodium dodecyl sulfate–polyacrylamide gel electrophoresis (Criterion, Bio-Rad). The gel was then fixed and stained with GelCode Blue (Pierce). The entire lane was cut, washed, reduced with DTT, alkylated with iodoacetamide, and digested with trypsin.

The peptides produced by this digestion were extracted with 50% methanol/10% formic acid in water and the extract dried and reconstituted in 1% acetic acid. The samples were analyzed using an *m/z* resolution of 140,000 with a hybrid quadrupole-orbitrap mass spectrometer (ThermoScientific Q-Exactive Plus) configured with a splitless capillary column HPLC system (ThermoScientific Ultimate 3000). The data were processed using the program Skyline (30), which determines the chromatographic peak areas for the selected peptides. The response for each protein was taken as the geometric mean of the response for the two peptides monitored for each protein. Changes in the relative abundance of the proteins were determined by normalization to the BSA internal standard, with confirmation by normalization to the housekeeping proteins. A list of the peptides used for the detection of proteins was reported previously (31).

Kinetic proteomics was performed using the Deuterater software package (32), which analyzes the deuterium-dependent change in the isotope pattern of each peptide in the full scan MS1 data. The same Q-Exactive data sets were analyzed for kinetics as were used for the quantitation. A database of mass, retention time, and sequence for each peptide of interest was assembled from LC-MS/MS peptide sequencing experiments on the same tissues using the same chromatography system. Representative LC-MS/MS runs at the time of the experiment confirmed that the accurate mass tag database could be applied. Each tissue was analyzed individually, but with all replicate tissues included for fitting of kinetics. Mass spectral accuracy was confirmed as less than 10% deviation from theory using peptides from the BSA internal standard. Precision filters for the kinetic fits of the deuterium-labeled peptides required a standard deviation of less than 10% for all internal deuterium incorporation metrics (33).

Statistics

Data are reported as mean ± SEM. Body, fat, and lean masses over time were analyzed as a two-way (treatment and time) ANOVA with Tukey's post hoc analysis. Tissue masses at necropsy were analyzed as reported previously (7). For quantitative proteomics, outlier data points were first removed by a ROUT (*Q* = 1%) outlier test. For all comparisons, significance was determined by a one-way ANOVA with Tukey's post hoc test and Benjamini–Hochberg false discovery rate correction (*q* = 5%). Statistical tests were performed and graphs generated using GraphPad Prism 7.0b for Mac OS X (GraphPad Software, La Jolla, CA). Heatmap and principal component analysis plot were generated using ClustVis with default settings (Row scaling = unit variance scaling, principal component analysis = SVD with imputation, clustering distance for rows = correlation, clustering method for rows = average, tree ordering for rows = tightest cluster first) (34).

Results

Body and Tissue Masses

The effect of treatments on body mass, fat mass, lean/fat mass ratios, calorie intake, and organ masses at necropsy was published previously (7). In brief, there was no significant effect of CR or 17α-E2 treatment on body mass, fat mass, or lean mass in the animals analyzed in these studies, but all groups displayed a significant effect of time on these variables (Figure 1). Despite not being

significant, CR and 17 α -E2 treatment did induce a downward trend in body mass, which is aligned with our previous report (7). During the period of D₂O administration (Figure 1, gray boxes), the pattern of changes in body mass and composition were generally the same as at the initiation of treatment. As reported previously (7), average heart, liver, skeletal muscle, inguinal WAT, and subscapular WAT masses were not different between groups, but epididymal WAT mass in 17 α -E2 and CR treatment groups was significantly different compared with CON (Table 1).

Proteostatic Outcomes by Tissue

We assessed rates of protein and DNA synthesis over a 2-week period as previously described for other long-lived models (18,20,21,25–27). The ratio of these two outcomes represents the contribution of protein synthesis for growth versus maintaining existing cellular structures (17,18). In non-adipose tissues, we further fractionated proteins into three protein fractions, including a mitochondrial fraction. There was little effect of treatment on the rates of protein synthesis, although there was a significant decrease in skeletal muscle mixed (primarily myofibrillar protein synthesis) with CR (Figure 2, first column). In our experience, during 2 weeks of labeling, liver proteins can be fully turned over thus requiring caution in the interpretation of these rates. Between tissues, there was a consistently slower rate of DNA synthesis with CR, but not 17 α -E2 (Figure 2, middle column), a finding consistent with lifelong CR (27). Of note, there were high rates of protein synthesis in WAT (Figure 2D–E). In addition, there was an effect of CR on proliferation within subcutaneous (Figure 2D), but not the epididymal WAT (Figure 2E), with no effect of 17 α -E2 on either depot. The ratio of protein to DNA synthesis increased with CR in heart and liver, whereas 17 α -E2 had no effect on any tissue (Figure 2, third column).

To further interrogate proteostatic outcomes, we used targeted proteomics to assess multiple metabolic and stress-responsive proteins in the aforementioned tissues. From these assessments, we were able to determine protein content, protein synthesis rates, absolute protein synthesis, and protein half-life (Supplemental File 2). A complete heat map of changes in protein content by tissue and targeted panel is presented in Figure 3A, with overall principal component analysis in Figure 3B and principal component analyses by tissue and targeted panel in Supplementary Figure 1A and B. These results suggest that there is no consistent difference in protein content of metabolic and stress response pathways across all tissues in response to treatment. However, changes in protein content were observed

for specific proteins in liver, subcutaneous WAT, and skeletal muscle due to treatment (Figure 3C–E). Generally speaking, CR significantly increased protein expression in liver whereas decreasing proteins in subcutaneous WAT. The effects of 17 α -E2 were less consistent, with some proteins being increased and others decreased in liver and subcutaneous WAT. Protein expression changes were mostly divergent between CR and 17 α -E2. Only EHHADH in liver and PRDX6 and HMGS2 in subcutaneous WAT exhibited the same response to both treatments.

The synthesis rates and half-lives of individual proteins are presented by tissue in Supplementary Figure 2A–E. In summary, with each treatment compared with CON, we plotted the Log₂ fold-change in protein fraction new (Figure 4) half-life (Supplementary Figure 3), or absolute synthesis (Supplementary Figure 3) versus Log₂ fold-change in protein content for proteins where both quantitative and kinetic values were available for all groups. Plotting in this manner suggests there is tissue specificity by which protein mass is regulated. For example, skeletal muscle displayed low variability in content but greater variability in synthesis rates, suggesting heterogeneity in regulation of protein content between tissues. Other tissues (eg, WATs) displayed equal variability of content and turnover rates. In general, CR and 17 α -E2 treatment groups clustered based on changes in content and synthesis, indicating that protein concentrations were regulated in a similar manner for both treatments. However, these groupings by treatment varied by tissue, indicating that there are likely tissue-specific differences in regulation of protein content.

Discussion

Understanding shared characteristics of long-lived models may provide insight into specific targets for slowing the aging process and increasing health span (35). We have previously demonstrated an increase in protein to DNA synthesis rates in multiple tissues from several long-lived models; thereby leading us to believe this is a shared characteristic of long life (17,18). In this study, we examined weight-matched old male mice undergoing short-term 17 α -E2 treatment or mild CR, with the expectation that like other treatments that curtail aging mechanisms, there would be improvements in proteostatic processes. To our surprise, after examining multiple tissues, including two previously unexplored WAT depots, we did not see the predicted differences in protein to DNA synthesis mechanisms following 17 α -E2 treatment. However, mild short-term CR (~18%) initiated at 20 months of age elicited differences consistent

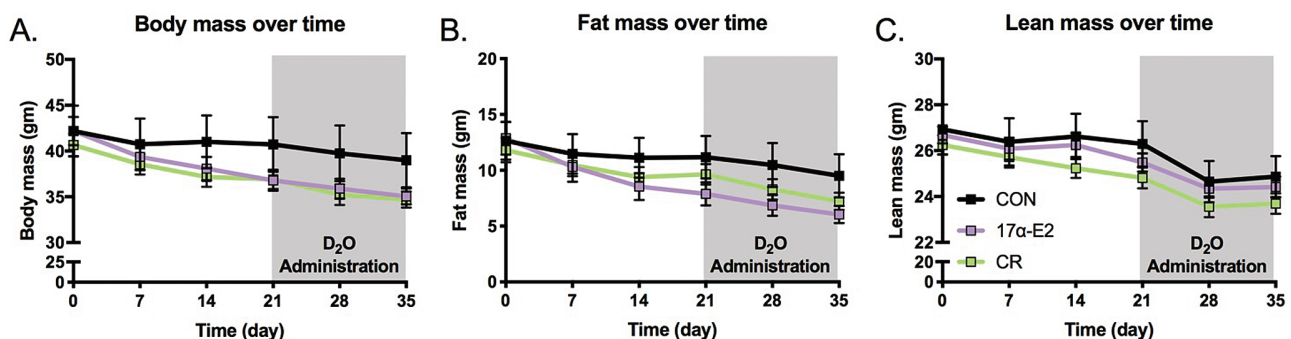


Figure 1. Changes in (A) body mass, (B) fat mass, and (C) lean mass over time in CON, 17 α -estradiol (17 α -E2), and caloric restriction (CR) treated mice. All groups displayed a significant effect of time on body mass, fat mass, and lean mass. The gray boxes along the x-axis represent the period of isotopic labeling and, therefore, the body mass conditions in which the proteostatic outcomes were determined. Values are presented as means \pm SEM. $n = 9$ (CON), 7 (CR), and 10 (17 α -E2).

Table 1. Body and Tissue Masses at Necropsy

	CON	17 α -E2	CR
Body mass (gm)	37.0 \pm 2.7	33.0 \pm 0.8	34.4 \pm 0.9
Non-adipose tissues			
Heart (mg)	170 \pm 9	171 \pm 4	164 \pm 6
Liver (mg)	1,564 \pm 191	1,439 \pm 29	1,325 \pm 33
Quadriceps (mg)	352 \pm 10	335 \pm 10	313 \pm 18
Intra-abdominal adipose tissue			
Epididymal WAT (mg)	1,631 \pm 261	1,006 \pm 141*	1,034 \pm 109*
Subcutaneous adipose tissue			
Inguinal WAT (mg)	1,011 \pm 288	633 \pm 149	766 \pm 113
Subscapular WAT (mg)	408 \pm 106	243 \pm 45	350 \pm 39

Note: Values are presented as means \pm SEM. $N = 9$ (CON), 10 (17 α -E2), and 7 (CR). * $p < .05$ versus CON. CR = caloric restriction; WAT = white adipose tissue; 17 α -E2 = 17 α -Estradiol.

with lifelong CR, rapamycin, and Protandim (Nrf2 activator) treatments (22,25). Further interrogation with targeted quantitative and kinetic proteomics did not resolve this unexpected finding. We, therefore, speculate that long-lived models that display growth and/or energy restriction induce synthetic responses that promote a mechanism of proteostasis, whereas 17 α -E2 likely extends health span and/or life span through alternative mechanisms.

One of the primary mechanisms for maintaining proteostasis is through changes in protein turnover. We have advocated that cell proliferation should be considered when determining the contribution of protein synthesis to proteostatic processes (17,18). Simultaneously assessing cell replication accounts for the amount of newly synthesized proteins that are directed toward maintenance of existing cells versus those required for growth. By using this approach, we have consistently demonstrated greater allocation of newly synthesized proteins toward somatic maintenance in multiple tissues following manipulations that increase life span and/or health span (17,18). To date, our laboratory has examined lifelong CR, rapamycin treatment, Snell dwarf mice, the crowded litter model, and Nrf2 activation with repeatable increases in the ratio of protein to DNA synthesis (18,20–22). Therefore, we have identified this trade-off between maintenance and proliferation (growth) as a potentially shared characteristic of slowed aging models in which energetic stress signaling is activated. We were surprised to find that 17 α -E2 treatment was an exception to this consistent and repeatable finding.

In this study, we examined mixed tissue proteins, cytosolic proteins, and mitochondrial proteins because in previous work, we have consistently observed protein fraction-specific (often mitochondrial) improvements in proteostatic mechanisms with slowed-aging interventions (17,18). Compared with CON, 17 α -E2 did not increase protein synthesis or proteostatic mechanisms in mitochondrial or any other protein fraction in any tissue analyzed. In addition, compared with CON, there was no significant difference in DNA synthesis with 17 α -E2, suggesting that short-term treatment with 17 α -E2 in late-life does not affect cellular proliferation. Most of our studies to date have been in slowed-aging models that restrict growth and/or inhibit cellular proliferation (20,27) or inhibit AMPK/mTOR signaling (25). Interestingly, we and others have established that chronic 17 α -E2 treatment does not modulate mTORC1 activity in liver (7,11), although we did find that 4 months of 17 α -E2 treatment in aged male mice increased AMPK activation and decreased mTORC1 signaling in epididymal WAT, which was paralleled by a significant loss of adiposity (7). Given that lean mass was maintained in this study, it suggests that the primary effects of 17 α -E2 are in WAT and potentially the hypothalamus as described elsewhere (10).

In the current analyses, we found that 17 α -E2 did not alter cell proliferation or proteostatic mechanisms in two different WAT depots despite the presence of an overall loss of adiposity. Previously, in tissues from this same cohort of mice, we demonstrated metabolic benefits that are associated with reductions in inflammation (7). Collectively, previous studies and our current study suggest that improvements in health span and/or longevity by 17 α -E2 are potentially due to positive metabolic outcomes, but not changes in proteostatic regulation. We speculate that sustained improvements in metabolic function may decrease the need for alterations in protein turnover to improve proteostasis, although additional studies are needed to confirm this speculation.

As opposed to 17 α -E2, 5 weeks of mild (~18%) CR at 20 months of age-induced changes in proteostatic mechanisms consistent with other life-long growth restricted models, including CR (17,18). These findings were unexpected and important for the potential translatability of alternative approaches to life-long CR. In heart, liver, and subcutaneous WAT, DNA synthesis rates were slower than CON, which is typically indicative of proliferative and/or growth restriction. Importantly, the magnitude of decrease in DNA synthesis in CR mice varied by tissue, indicating that decreased proliferation was not simply due to one factor such as cells of hematopoietic origin (eg, macrophage). The greater ratio of protein to DNA synthesis in CR mice suggests enhanced proteostatic processes contributing to somatic maintenance across tissues and typically in more than one protein fraction. In a previous report, we found greater proteostatic mechanisms in life-long, 40% calorically restricted mice compared with ad libitum fed mice (18). In this study, we also found that compared with CON, the number of differentially expressed proteins with CR far exceeded that of 17 α -E2 treatment. These data add to the growing evidence that the positive effects of CR can be induced with much less severe restriction and/or duration (36–40). In addition, these findings also indicate that CR can be initiated later in life with potential benefits on health span. Therefore, it seems apparent that despite a similar maintenance of body mass, 17 α -E2 and CR treatments elicit distinctly different proteostatic outcomes.

To further explore proteostatic processes, we used a targeted proteomics approach to measure both protein content and protein synthesis. Included in our analyses were panels of proteins related to carbohydrate metabolism, fatty acid metabolism, stress responses, TCA cycle, and housekeeping proteins (Supplementary File 1). For the proteins analyzed, there were few significant differences in protein content between treatments. However, and important to the potential beneficial effects of a slowed-aging treatment, the rates of synthesis varied to a greater degree than protein content, indicating

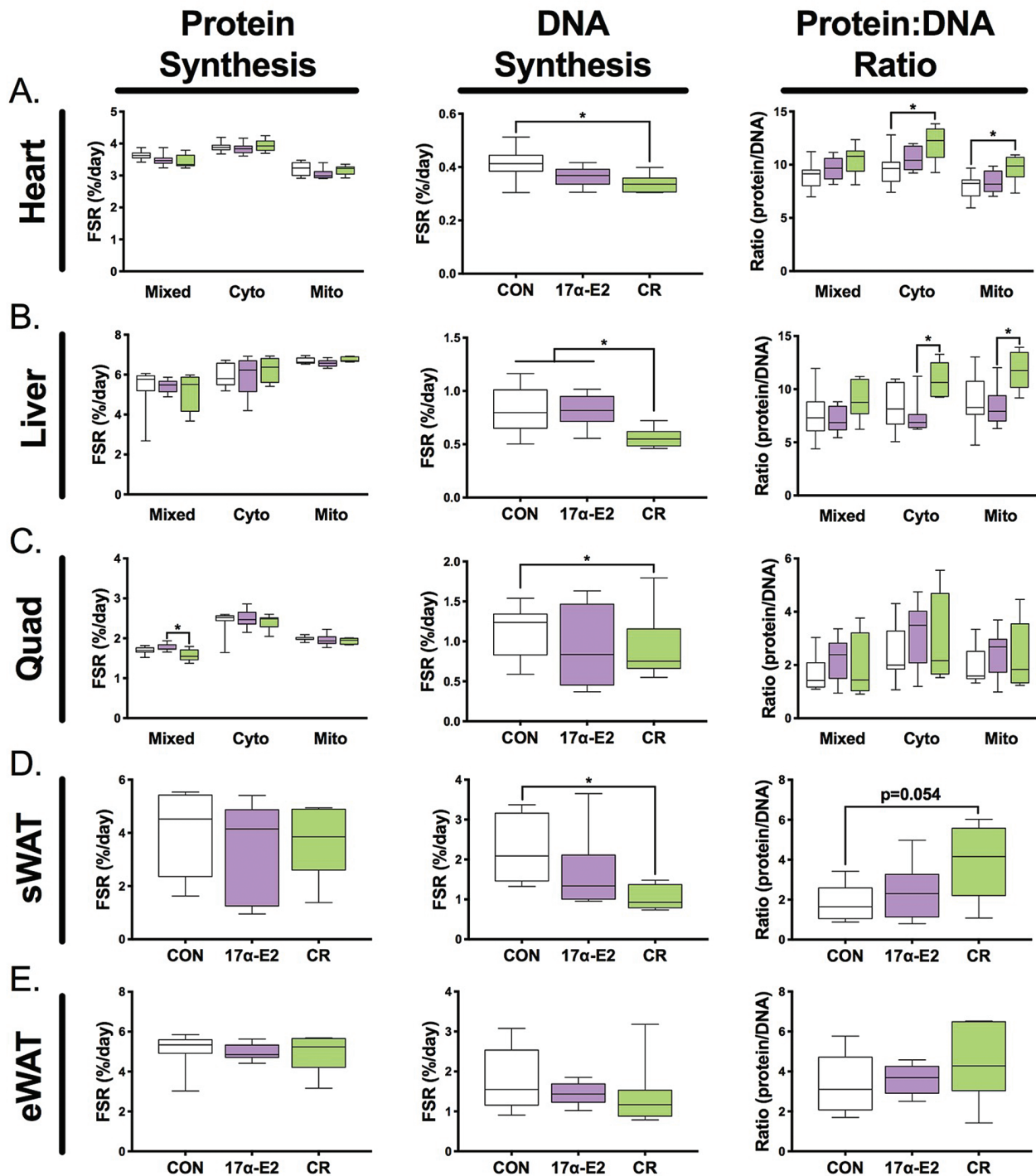


Figure 2. Proteostatic mechanisms in the: (A) heart, (B) liver, (C) skeletal muscle, (D) subcutaneous WAT (inguinal), and (E) epididymal white adipose tissue (WAT) depots as assessed by protein synthesis (left column), DNA synthesis (middle column), and the protein/DNA synthesis ratio (right column). Rates were determined using D_2O labeling over 2 weeks. Values are presented as means \pm SEM. $n = 7-9$ (CON), $5-6$ (CR), and $9-10$ (17α -E2). $*p < .05$ for each comparison. CR = caloric restriction; 17α -E2 = 17α -estradiol.

that solely measuring protein content does not accurately represent proteostatic and other dynamic processes (41). Figure 4 illustrates that the relationship between protein content and protein turnover tends to group by tissue, rather than treatment. These data illustrate that there may be tissue-specific processes regulating protein content and proteostasis. For example, in tissues like skeletal muscle and

heart, energetic demands vary throughout the day and can change by orders of magnitude in short periods of time (eg, during exercise). In other tissues such as liver, energetic demands are relatively constant. Because energy on demand for one cellular process compromises that for another (eg, energetically expensive process of protein synthesis) the regulation of protein turnover and content may vary between

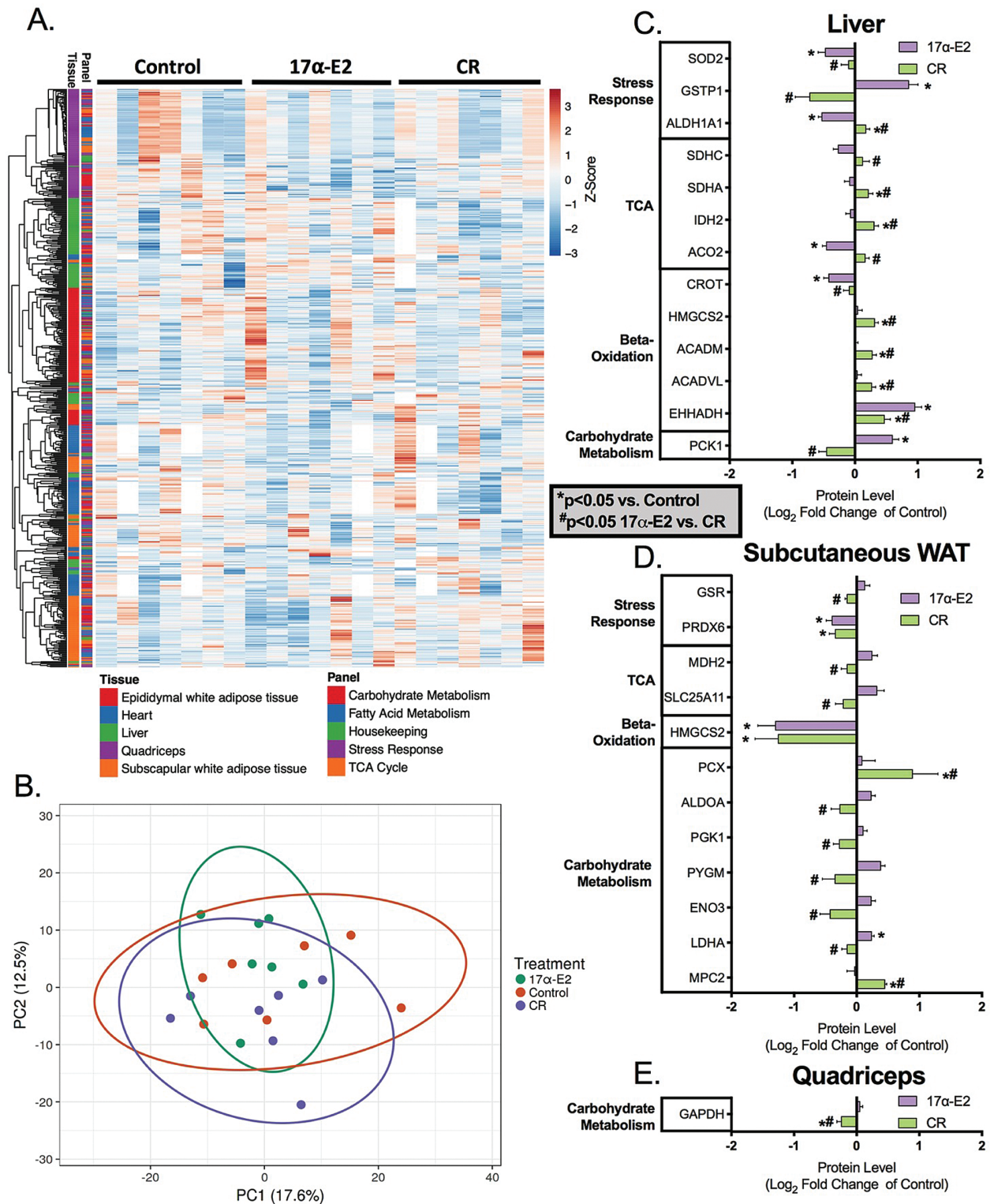


Figure 3. (A) Protein content in epididymal white adipose tissue (WAT), heart, liver, skeletal muscle, and subcutaneous WAT (subscapular). Not all samples were run for all tissues, therefore, white values represent missing data. (B) Principal component analysis for protein content of all tissues and panels. Proteins with significant changes in content for both treatments in (C) liver, (D) subcutaneous WAT (subscapular), and (E) skeletal muscle in response to 17 α -estradiol (17 α -E2) and caloric restriction (CR). Protein content was determined using targeted mass spectrometry. Values are represented as mean log₂ fold-change \pm SEM relative to CON. $n = 7$ (CON), 7 (CR), and 6–7 (17 α -E2). * $p < .05$ versus CON, # $p < .05$ 17 α -E2 versus CR.

tissue types. Although it is not possible to address this question in this study, the data indicate that a slowed-aging treatment changes protein dynamics in a tissue-specific manner. In this study, there were

limited numbers of proteins for which both content and synthesis were available necessitating future studies to further explore tissue-related differences in proteostatic mechanism.

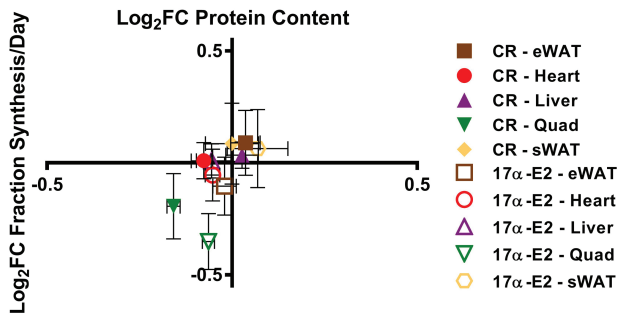


Figure 4. Change fractional synthesis/day (y-axis) versus change in protein content (x-axis). Each protein is represented as \log_2 fold-change relative to CON means \pm SEM for each tissue. $n = 5-7$ (CON), $6-7$ (CR), and $6-7$ (17α -E2).

There are a few notable limitations to this study. First, tracer measured proteostatic outcomes were initiated 3 weeks after initiating treatments. Therefore, it is plausible that proteostatic remodeling occurred in the early treatment phase, which led to a reduced need for remodeling in the latter period. We speculate this could be especially true in the case of 17α -E2 treatment, where robust metabolic changes occur in the first few weeks of administration (7,10). We justified our approach to labeling because it captured steady-state conditions that are relevant during long-term treatment. Second, there were limited proteins for which both synthesis and content were measured. This limitation was due to the complexity of measuring label incorporation into peptides (32). Third, it is possible that given the appearance of potential trends in the differences of ratios between 17α -E2 and CON, that the 17α -E2 group was underpowered. However, power calculations indicated that an n of 19–84 mice (depending on fraction) would be required for a p value of less than 0.05 and a power of 0.80. Therefore, we do not believe that the study was underpowered. Finally, these studies were only performed in male mice, and thus, no conclusions can be drawn with regard to potential relationships among CR, 17α -E2, proteostasis, and life span-extension in females. It must also be noted that our isotope studies and quantitative proteomics were performed in two different subcutaneous WAT depots, which may possess mildly different metabolic profiles. In contrast, the strengths of the study were the consideration of cell proliferation when accounting for protein synthesis, the measurement of five tissues including the first description of two WAT depots, and the novel simultaneous analysis of protein content and synthesis rates for the determination of proteostatic mechanisms.

We conclude that as opposed to multiple growth and energy restricted models, and contrary to our initial hypothesis, 17α -E2 treatment in male mice does not increase the contribution of protein synthesis to proteostatic processes. However, we demonstrate that mild, short-term CR initiated in older male mice induces changes consistent with life-long 40% CR and other long-lived models that are growth or energy restricted. This finding supports the growing body of literature supporting practical and translatable modifications of traditional life-long CR to increase feasibility in human subjects. Finally, the combination of targeted and quantitative proteomics shed light on potential tissue-specific mechanisms to modulate proteostasis, a finding that needs to be more fully explored.

Supplementary Material

Supplementary data are available at *The Journals of Gerontology, Series A: Biological Sciences and Medical Sciences* online.

Funding

This work was supported by the National Institutes of Health (R01 AG042569 to B.F.M. and K.L.H., R00 AG51661 to M.B.S., and T32 AG052363 to S.N.M.) and Pilot Research Funding from the Oklahoma Nathan Shock Center of Excellence in the Basic Biology of Aging (M.B.S.).

Acknowledgments

We would like to acknowledge the assistance of Justin Reid, Sarah Ehrlicher, Gaia Bublitz, Kim Cox-York, and Tamar Pirtskhalava.

Conflict of Interest

The authors have no conflict of interest to declare.

References

- Fontana L, Partridge L. Promoting health and longevity through diet: from model organisms to humans. *Cell*. 2015;161:106–118. doi: 10.1016/j.cell.2015.02.020
- Nadon NL, Strong R, Miller RA, Harrison DE. NIA interventions testing program: investigating putative aging intervention agents in a genetically heterogeneous mouse model. *EBioMedicine*. 2017;21:3–4. doi: 10.1016/j.ebiom.2016.11.038
- Anstead GM, Carlson KE, Katzenellenbogen JA. The estradiol pharmacophore: ligand structure-estrogen receptor binding affinity relationships and a model for the receptor binding site. *Steroids*. 1997;62:268–303.
- Littlefield BA, Gurside E, Markiewicz L, McKinley B, Hochberg RB. A simple and sensitive microtiter plate estrogen bioassay based on stimulation of alkaline phosphatase in Ishikawa cells: estrogenic action of delta 5 adrenal steroids. *Endocrinology*. 1990;127:2757–2762. doi: 10.1210/endo-127-6-2757
- Harrison DE, Strong R, Allison DB, et al. Acarbose, 17α -estradiol, and nordihydroguaiaretic acid extend mouse lifespan preferentially in males. *Aging Cell*. 2014;13:273–282. doi: 10.1111/acel.12170
- Strong R, Miller RA, Antebi A, et al. Longer lifespan in male mice treated with a weakly estrogenic agonist, an antioxidant, an α -glucosidase inhibitor or a Nrf2-inducer. *Aging Cell*. 2016;15:872–884. doi: 10.1111/acel.12496
- Stout MB, Steyn FJ, Jurczak MJ, et al. 17α -Estradiol alleviates age-related metabolic and inflammatory dysfunction in male mice without inducing feminization. *J Gerontol A Biol Sci Med Sci*. 2017;72:3–15. doi: 10.1093/gerona/glv309
- Johnson SC, Rabinovitch PS, Kaeberlein M. mTOR is a key modulator of ageing and age-related disease. *Nature*. 2013;493:338–345. doi: 10.1038/nature11861
- Salminen A, Kaarniranta K. AMP-activated protein kinase (AMPK) controls the aging process via an integrated signaling network. *Ageing Res Rev*. 2012;11:230–241. doi: 10.1016/j.arr.2011.12.005
- Steyn FJ, Ngo ST, Chen VP, Bailey-Downs LC, Xie TY, Ghadami M, et al. 17α -estradiol acts through hypothalamic pro-opiomelanocortin expressing neurons to reduce feeding behavior. *Aging Cell*. 2018;17(1). doi: 10.1111/acel.12703.
- Garratt M, Bower B, Garcia GG, Miller RA. Sex differences in lifespan extension with acarbose and 17α estradiol: gonadal hormones underlie male-specific improvements in glucose tolerance and mTORC2 signaling. *Aging Cell*. 2017;16:1256–1266. doi: 10.1111/acel.12656
- Kennedy BK, Lamming DW. The mechanistic target of rapamycin: the grand ConducTOR of metabolism and aging. *Cell Metab*. 2016;23:990–1003. doi: 10.1016/j.cmet.2016.05.009
- Garratt M, Lagerborg KA, Tsai YM, Galecki A, Jain M, Miller RA. Male lifespan extension with 17α -estradiol is linked to a sex-specific metabolomic response modulated by gonadal hormones in mice. *Aging Cell*. 2018;e12786. doi: 10.1111/acel.12786

14. Kirkwood TB, Holliday R. The evolution of ageing and longevity. *Proc R Soc Lond B Biol Sci.* 1979;205:531–546. doi: 10.1098/rspb.1979.0083
15. López-Otín C, Blasco MA, Partridge L, Serrano M, Kroemer G. The hallmarks of aging. *Cell.* 2013;153:1194–1217. doi: 10.1016/j.cell.2013.05.039
16. Kennedy BK, Berger SL, Brunet A, et al. Geroscience: linking aging to chronic disease. *Cell.* 2014;159:709–713. doi: 10.1016/j.cell.2014.10.039
17. Hamilton KL, Miller BF. Mitochondrial proteostasis as a shared characteristic of slowed aging: the importance of considering cell proliferation. *J Physiol.* 2017;595:6401–6407. doi: 10.1113/jp274335
18. Miller BF, Drake JC, Naylor B, Price JC, Hamilton KL. The measurement of protein synthesis for assessing proteostasis in studies of slowed aging. *Ageing Res Rev.* 2014;18:106–111. doi: 10.1016/j.arr.2014.09.005
19. Barbet NC, Schneider U, Helliwell SB, Stansfield I, Tuite MF, Hall MN. TOR controls translation initiation and early G1 progression in yeast. *Mol Biol Cell.* 1996;7(1):25–42.
20. Drake JC, Bruns DR, Peelor FF 3rd, et al. Long-lived Snell dwarf mice display increased proteostatic mechanisms that are not dependent on decreased mTORC1 activity. *Aging Cell.* 2015;14:474–482. doi: 10.1111/ace.12329
21. Drake JC, Bruns DR, Peelor FF 3rd, et al. Long-lived crowded-litter mice have an age-dependent increase in protein synthesis to DNA synthesis ratio and mTORC1 substrate phosphorylation. *Am J Physiol Endocrinol Metab.* 2014;307:E813–E821. doi: 10.1152/ajpendo.00256.2014
22. Bruns DR, Ehrlicher SE, Khademi S, et al. Differential effects of vitamin C or protandim on skeletal muscle adaptation to exercise. *J Appl Physiol (1985).* 2018;125:661–671. doi: 10.1152/jappphysiol.00277.2018
23. Stout M, Tchkonja T, Kirkland J. The aging adipose organ: lipid redistribution, inflammation, and cellular senescence. In: Fantuzzi G, Braunschweig C, eds. *Adipose Tissue and Adipokines in Health and Disease.* Nutrition and Health: New York, NY: Humana Press; 2014:69–80.
24. Stout MB, Justice JN, Nicklas BJ, Kirkland JL. Physiological aging: links among adipose tissue dysfunction, diabetes, and frailty. *Physiology (Bethesda).* 2017;32:9–19. doi: 10.1152/physiol.00012.2016
25. Drake JC, Peelor FF III, Biela LM, et al. Assessment of mitochondrial biogenesis and mTORC1 signaling during chronic rapamycin feeding in male and female mice. *J Gerontol A Biol Sci Med Sci.* 2013;68:1493–1501. doi: 10.1093/gerona/glt047
26. Miller BF, Robinson MM, Reuland DJ, et al. Calorie restriction does not increase short-term or long-term protein synthesis. *J Gerontol A Biol Sci Med Sci.* 2013;68:530–538. doi: 10.1093/gerona/gls219
27. Miller BF, Robinson MM, Bruss MD, Hellerstein M, Hamilton KL. A comprehensive assessment of mitochondrial protein synthesis and cellular proliferation with age and caloric restriction. *Aging Cell.* 2012;11:150–161. doi: 10.1111/j.1474-9726.2011.00769.x
28. Busch R, Kim YK, Neese RA, et al. Measurement of protein turnover rates by heavy water labeling of nonessential amino acids. *Biochim Biophys Acta.* 2006;1760:730–744. doi: 10.1016/j.bbagen.2005.12.023
29. Busch R, Neese RA, Awada M, Hayes GM, Hellerstein MK. Measurement of cell proliferation by heavy water labeling. *Nat Protoc.* 2007;2:3045–3057. doi: 10.1038/nprot.2007.420
30. MacLean B, Tomazela DM, Shulman N, Chambers M, Finney GL, Frewen B, et al. Skyline: an open source document editor for creating and analyzing targeted proteomics experiments. *Bioinformatics.* 2010;26:966–968. doi: 10.1093/bioinformatics/btq054
31. Bhaskaran S, Unnikrishnan A, Ranjit R, et al. A fish oil diet induces mitochondrial uncoupling and mitochondrial unfolded protein response in epididymal white adipose tissue of mice. *Free Radic Biol Med.* 2017;108:704–714. doi: 10.1016/j.freeradbiomed.2017.04.028
32. Naylor BC, Porter MT, Wilson E, et al. Deuterater: a tool for quantifying peptide isotope precision and kinetic proteomics. *Bioinformatics.* 2017;33:1514–1520. doi: 10.1093/bioinformatics/btx009
33. Mathis AD, Naylor BC, Carson RH, et al. Mechanisms of in vivo ribosome maintenance change in response to nutrient signals. *Mol Cell Proteomics.* 2017;16:243–254. doi: 10.1074/mcp.M116.063255
34. Metsalu T, Vilo J. ClustVis: a web tool for visualizing clustering of multivariate data using principal component analysis and heatmap. *Nucleic Acids Res.* 2015;43(W1):W566–W570. doi: 10.1093/nar/gkv468
35. Huffman DM, Justice JN, Stout MB, Kirkland JL, Barzilai N, Austad SN. Evaluating health span in preclinical models of aging and disease: guidelines, challenges, and opportunities for geroscience. *J Gerontol A Biol Sci Med Sci.* 2016;71:1395–1406. doi: 10.1093/gerona/glw106
36. Brandhorst S, Choi IY, Wei M, et al. A periodic diet that mimics fasting promotes multi-system regeneration, enhanced cognitive performance, and healthspan. *Cell Metab.* 2015;22:86–99. doi: 10.1016/j.cmet.2015.05.012
37. Martinez-Lopez N, Tarabra E, Toledo M, et al. System-wide benefits of intermeal fasting by autophagy. *Cell Metab.* 2017;26:856–871.e5. doi: 10.1016/j.cmet.2017.09.020
38. Mitchell SJ, Madrigal-Matute J, Scheibye-Knudsen M, et al. Effects of sex, strain, and energy intake on hallmarks of aging in mice. *Cell Metab.* 2016;23:1093–1112. doi: 10.1016/j.cmet.2016.05.027
39. Xie K, Neff F, Markert A, et al. Every-other-day feeding extends lifespan but fails to delay many symptoms of aging in mice. *Nat Commun.* 2017;8:155. doi: 10.1038/s41467-017-00178-3
40. Richardson A, Austad SN, Ikeno Y, Unnikrishnan A, McCarter RJ. Significant life extension by ten percent dietary restriction. *Ann N Y Acad Sci.* 2016;1363:11–17. doi: 10.1111/nyas.12982
41. Miller BF, Hamilton KL. A perspective on the determination of mitochondrial biogenesis. *Am J Physiol Endocrinol Metab.* 2012;302:E496–E499. doi: 10.1152/ajpendo.00578.2011